Alexandria Engineering Journal (2020) 59, 1135–1147

HOSTED BY

ELSEVIER

Alexandria University

Alexandria Engineering Journal

www.elsevier.com/locate/aej
www.sciencedirect.com

ORIGINAL ARTICLE

Grasping force prediction based on sEMG signals

Ruyi Ma [a,b], Leilei Zhang [a,b], Gongfa Li [b,c,*], Du Jiang [c,d], Shuang Xu [c,d], Disi Chen [e]

[a] *Key Laboratory of Metallurgical Equipment and Control Ministry of Education, Wuhan University of Science and Technology, Wuhan 430081, China*
[b] *Institute of Precision Manufacturing, Wuhan University of Science and Technology, Wuhan 430081, China*
[c] *Research Center of Biomimetic Robot and Intelligent Measurement and Control, Wuhan University of Science and Technology, Wuhan 430081, China*
[d] *Hubei Key Laboratory of Mechanical Transmission and Manufacturing Engineering, Wuhan University of Science and Technology, Wuhan 430081, China*
[e] *School of Computing, University of Portsmouth, Portsmouth PO1 3HE, UK*

Received 13 November 2019; revised 26 December 2019; accepted 3 January 2020
Available online 16 January 2020

KEYWORDS

sEMG;
Gene expression programming algorithm;
Force prediction;
Pattern recognition

Abstract In order to realize the force control, when the prosthetic hand grasps the object, the forearm electromyography signal is collected by the multi-channel surface electromyography (sEMG) acquisition system. The grasping force information of the human hand is recorded by the six-dimensional force sensor. The root mean square (RMS) of the electromyography signal steady state is selected, which is an effective feature. The gene expression programming algorithm (GEP) and BP neural network are used to construct the prediction model and predict the grasping force. The force prediction accuracy of GEP algorithm and BP neural network algorithm are discussed under different grasping power levels and different grasping modes. The performance of the two algorithm models are evaluated by two measures of root mean square error (RMSE) and correlation coefficient (CC). The results show that the RMS eigenvalue extracted from the sEMG signal can better characterize the grasping force. The prediction model with GEP algorithm has smaller relative error and higher prediction effect.

1. Introduction

Artificial intelligence is a very hot topic nowadays. The rapid development of robot technology has been promoting the expansion of the application field of artificial intelligence. The application field of artificial intelligence has expanded from industrial production to medical, service and military fields. The core of artificial intelligence is the design of algorithm. At present, there are a large number of researchers in the study of how to solve the design algorithm and the realization of new computing methods. In this paper, GEP and BP neural network are combined to build the prediction model and predict the grasping force, so as to get the application of sEMG signals [1–3].

The sEMG is an electrical signal generated by evaluating and recording muscle contraction. It contains abundant

* Corresponding author at: Institute of Precision Manufacturing, Wuhan University of Science and Technology, Wuhan 430081, China.
E-mail address: ligongfa@wust.edu.cn (G. Li).

Peer review under responsibility of Faculty of Engineering, Alexandria University.

https://doi.org/10.1016/j.aej.2020.01.007
1110-0168

physiological motion information and reflects people's motor intentions [4]. As the bioelectrical signals of the human body, the sEMG is an ideal source of human biosignal control that can be widely used [5–8]. By analyzing and processing the sEMG, the human hand movement mode can be recognized [9], but it is difficult to accurately control the output force of the prosthetic hand. How to dig out the force information in the electromyography signals (EMG) to improve the flexible control of the prosthetic hand is a difficult problem to be solved. The action of the prosthetic hand can be controlled by detecting the bioelectrical signals generated by the corresponding muscles of the human body [10,11]. This artificial hand controlled by the electrical signals generated by the corresponding muscles is called electromyography artificial hand [12]. Since the EMG is a bioelectrical signal generated when the human neuromuscular system is active, the electromyography artificial hand and the real human hand belong to the same homologous control. Therefore, the EMG is an ideal signal source for the human-computer interaction system [13,14].

Traditional methods based on EMG signals driving force estimation often require extraction of muscle activation. However, due to the randomness and variability of EMG signals, the degree of muscle activation is difficult to obtain accurately [15–17]. Furthermore, the transformation from muscle activation to muscle strength depends on some phenomena models, such as the Huxley model and the Hills model [18]. At present, although the myoelectric artificial hand control can meet the requirements of intuitive control, there is still no good solution to the synchronous control of multi-degree of freedom grasping mode and grasping force [19,20]. In recent years, sEMG have received great attention as a source of control for prosthetic limbs and intelligent exoskeletons [21]. And advanced control techniques such as pattern recognition technology [22] and regression techniques have been rapidly development of. However, due to the practical limitations of different positions or movements of the arm, electrode displacement, non-stationary signals, and changes in force, the clinical application of prosthetic and exoskeleton based on sEMG are still affected. And a good user experience cannot be achieved [23,24]. The high recognition rate in the literature reports is often obtained in a strictly controlled experimental environment, which leads to serious imbalances in scientific research results and clinical applications [25–27]. Among the many factors affecting the stability of EMG, the magnitude of the grasping force causes a significant change in the characteristics of the ENG, which leads to a decrease in the recognition rate of the grasping action. 16-channel electrode sleeves are used to collect human EMG. Compared with traditional sENG, it is expected to solve the problem of grasping force independent of muscle dynamics and muscle localization. And it has good universality.

The innovation of this paper is to construct a grasping force prediction model which is based on Gene Expression Programming (GEP) algorithm. Compared with BP neural network prediction model, the prediction error of grasping force based on GEP prediction model is smaller and the correlation coefficient is higher.

The rest is organized as follows. In Section 2, the related works on grasping force prediction method are introduced. The signals acquisition is described in Section 3. Section 4 introduces the proposed algorithm. Section 5 contains experimental results and the discussion of experimental results. The conclusion is in Section 6.

2. Related works

Castellini et al. of AI Data Laboratory in Munich have studied the recognition of grasping force and grasping action respectively [28]. The recognition rate of action is 89.7%, and the error of force estimation is 7.9% [29]. Lioyd et al. have studied the method of predicting muscle strength and knee joint moment by acquiring EMG signals and joint muscle parameters under different dynamic contraction conditions [30]. The method uses three-dimensional anatomical model which are improved Hill muscle model, discrete non-linear EMG signals model and calibration model respectively. The final determination coefficient of knee joint moment and measurement value is 0.91 ± 0.04. Gagnon et al. proposed an improved multi-joint electromyography-assisted optimization method to estimate the joint force in the lumbar musculoskeletal model [31,32]. The objective function was found to estimate the muscle force under the condition of lumbar joint balance. This study is helpful to further explore the relationship between human muscles and joint movements, but intrusive methods need to obtain the characteristic parameters of muscles and bones, which will bring some pain to the experimenters. From the physiological point of view, muscle contraction force is mainly expressed by the size and frequency of human action potential. These parameters can be obtained by measuring sEMG signals. These parameters can be further studied to make use of the correlation between sEMG signals and muscle contraction force [33,34].

Many scholars have also conducted research on the effects of changes in force and the robustness control of myoelectric prostheses. Scheme et al. suggested that the intensity of motion at different levels of force may vary greatly from one another [35,36]. Al-Timemy et al. also pointed out that the change of force may lead to a 60% reduction in the accuracy of EMG control system [37]. Subsequently, they studied the problem of robust control of hand prosthesis under the condition of force level change, and found that force change may have a greater impact on the robustness of prosthesis control [38]. Although stability control can be improved by increasing training samples, it will lead to more complex classifier, longer training process and lower classification accuracy.

At present, most studies need to establish the relationship between muscle strength and EMG signals based on muscle model. But the complexity and uncertainty of human physiological structure, individual differences in different people make it difficult to establish an accurate force estimation model. In addition, as far as the acquisition device is concerned, when the conventional device collects signals for a long time, the position of the electrode is liable to change and shift, which reduces the reliability of the EMG signals and the accuracy of the influence prediction.

Through the introduction of the relevant research status of sEMG, we can find that a lot of scholars have done a lot of work on sEMG research. But there is still no convincing method or norm on how to accurately predict the catch and get high accuracy. There are still ambiguities about many of the details of the specific processing of sEMG. In order to obtain higher grasping accuracy, it is necessary to systematically study the surface EMG signal. The research carried out in this experiment is of great significance.

The main reasons for the research on grasping force prediction from the aspects of sEMG are as follows:

As the human body's own biological signals, the sEMG contain a wealth of human body motion information. There are relatively mature processing algorithms and theories in software, and some successful application cases on the hardware. The sEMG signals acquisition method is simple to operate and does not cause extra trauma to the human body. So it can be an ideal signal source.

The sEMG signal is a bioelectrical signal formed by muscle contraction, so the control of the action of the central nervous system on the human body is directly related to the EMG signal. For people with amputation or limb disability leading to muscle dysfunction, it is hoped that by controlling the prosthetic hand, different action modes can be used to grasp objects of different shapes and weights. This practical need is expected to be achieved by further mining human motion information contained in sEMG signals.

The sleeve can collect sEMG signals conveniently and real-time, without considering the specific muscle location corresponding to human movement. It can operate and use rehabilitation equipment such as prosthetic hand better. It is also the advantage of the future development of the application of sEMG signals.

3. Multi-channel EMG signals acquisition

3.1. EMG signals acquisition device

EMG signals acquisition device has ELONXI electromyograph and electrode sleeve. The integrated dual Bluetooth module is sent to the PC-side Bluetooth port to provide data for the matching acquisition and analysis software MyoAnalytics. The grasping force is collected by a six-dimensional force sensor acquisition system. The grasping force data is collected by the two acting faces of the pinch pressure sensor. The acquisition system is shown in Fig. 1.

3.2. Manual capture mode selection

Because of the complex structure of the hand, more degrees of freedom and various combinations of finger joint movements, the hand can achieve a variety of grasping movements. Literatures have studied the grasping maneuvers in daily life, and summarized six basic grasping modes: cylindrical, fingertip, hook, palmar, spherical and lateral [39,40]. Through the above six kinds of grasping modes, the human hand can complete most of the actions of grasping objects in daily life. Considering the simple usage of movements and the feasibility of pattern recognition, four grasping modes are selected, namely, G1 for thumb and index finger, G2 for thumb and middle finger, G3 for thumb three finger and G4 for thumb five finger, as shown in Fig. 2.

3.3. Experimentation object and process

3.3.1. Experimental subjects

Three healthy males, 22–27 years old, were selected for the study. There was no history of neurological or musculoskeletal. And written informed consent was given to the subjects. The subjects were in a normal indoor environment without large equipment and serious noise interference. In order to collect accurate and effective EMG signals, the subjects did not exercise vigorously before the collection experiment, with keeping the muscles naturally relaxed and avoiding the effects of muscle fatigue on the EMG signals.

3.3.2. Experiment process

Wearing the surface electrode sleeve and using the alcohol cotton to wipe the subject's arm with alcohol should be in accordance with the experimental requirements. On the one hand, it can clean the dirt and cuticle on the skin surface to reduce the skin impedance. On the other hand, it can increase the skin's electrical conductivity and improve electrical and mechanical contact of the electrodes. Before starting to collect signals, the subject first performs familiar training according to the experimental grasping action, and detects whether the acquisition system hardware is running normally.

The maximum autonomous contraction experiment was conducted. The maximum grasping force was generated by increasing the force to the maximum within 5 s and keeping it for 5 s. The maximum amplitude of EMG signals and the corresponding grasping force were recorded as the reference values for normalization of EMG data.

Hand grasping can be divided into the following four modes: G1 for thumb and index finger, G2 for thumb and middle finger, G3 for thumb three finger and G4 for thumb five finger. Subjects were set to a frequency of 100 Hz in different capture modes. The finger grasped the upper and lower contact faces of the six-dimensional force sensor for 5 s continuous force pinching, and gradually changed the grasping force. The mean value of the 100% maximum voluntary contraction (MVC) was used as a reference value for calculating the magnitude of the grading force. We have used common levels. From 0% to 100% of MVC (20%, 40%, 60%, 80%) [41], the grasping force was 0–90 N.

The experiment was divided into four groups according to the above four capture modes, and the data was repeatedly collected four times. In each group, the G1–G4 grasping mode was sequentially performed. After the force signals was collected in each group of grasping modes, the subject rested for 5 min to rest the forearm muscle group to prevent muscle fatigue. During the whole experiment, attention should be paid to avoiding removing or moving the position of the electrode sleeve. And the position of the surface electrode should be kept as constant as possible

3.4. Feature selection of EMG signals

There are three main methods for analyzing the sEMG signals: time domain feature analysis, frequency domain feature analysis and time-frequency domain feature analysis [42–44]. Most of the features can be used to characterize changes in sEMG signals, and the magnitude of the grasping force is directly related to the magnitude of the sEMG signals [45–47]. Therefore, the choice of features directly affects the accuracy of the results of the grasping prediction. If multiple types of features are used at the same time, the amount of calculation will be increased, causing delay, which will bring a heavy burden to the subsequent algorithm construction. And the feature selection method will not always extract the most effective EMG

Fig. 1 Experimental acquisition system.

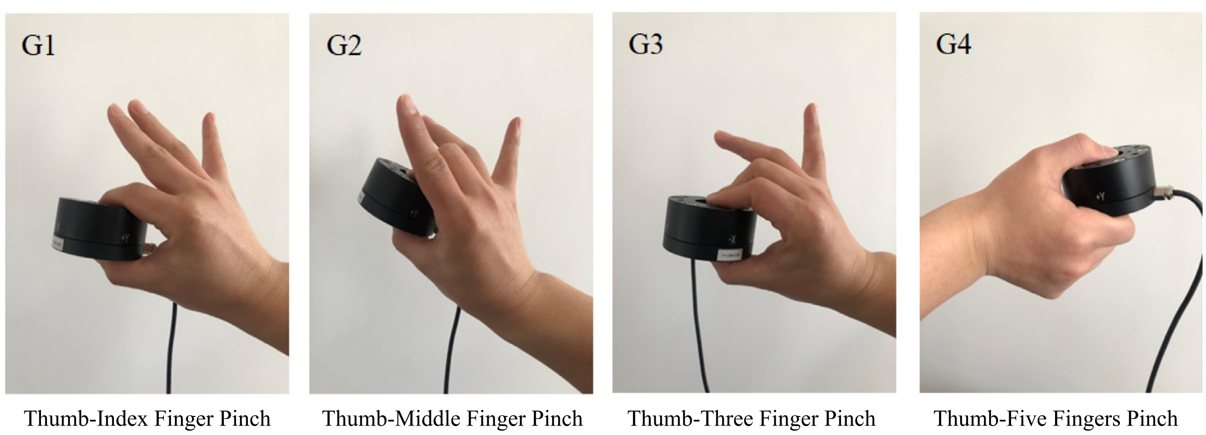

Fig. 2 Four grasping modes selected.

signals characteristics. The time domain features and frequency domain features calculated based on the sEMG signals amplitude do not need to undergo Fourier transform, and the calculation is simple [48,49]. Considering the minimization of the amount of computation and the redundancy of data information, the representative single-featured RMS performance capability was studied [50–52].

A set of experimental data was selected to segment the synchronous EMG signals data samples from 0% MVC to 80% MVC. The time window size was set to 200 ms and the step length was set to 100 ms. The RMS was calculated and the average value was selected to represent the change level of pattern recognition and grasping force of grasping action. The mean value of RMS characteristics of sEMG signals under four grasping maneuvers is shown in Figs. 3–6.

It can be seen from Figs. 3–6 that for the same grasping mode, different levels of grasping force are 20%, 40%, 60%, 80% (MVC). The magnitude of RMS of EMG signals in each channel is obviously different, and it will increase with the increase of grasping force. It shows that the time domain characteristics of sEMG signals are directly related to the human hand grasping action, and can be used to characterize the grasping force. Therefore, the RMS can reflect the amplitude change characteristics of sEMG signals in time dimension, which can be used to measure muscle activity in real time and nondestructively. At the same time, this feature algorithm is simple, convenient, less computational complexity and strong real-time. After comprehensive consideration, RMS feature is selected as the main feature of grasping force prediction model.

4. Proposed algorithm

4.1. Data processing

In order to reduce the amount of calculation and improve the response speed of the system, considering the standardization

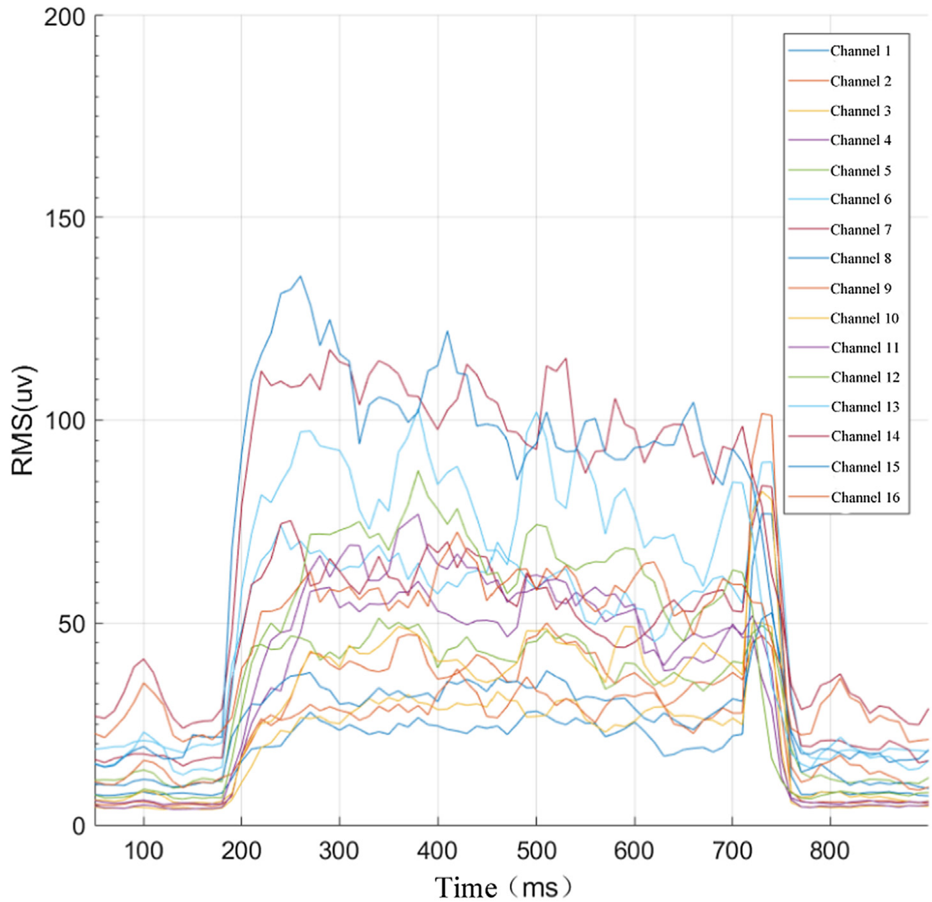

Fig. 3 20%MVC.

methods and their properties, the experimental data standardization method adopts the corresponding maximum value of the same eigenvalue as the reference. And the remaining data is used as a reference. Standardization is performed as shown in Eq. (1).

$$y_j = \frac{x_i - x_{\min}}{x_{\max} - x_{\min}} \tag{1}$$

where x_i is the original sEMG signals. y_i is the sEMG signals after normalization. $x_{\min}$ and $x_{\max}$ are the minimum and maximum values of x_i respectively.

The EMG signals data is defined as a vector of one-dimensional 16 elements, each element corresponding to a sample value of one channel.

$$X = [x_1, x_2, x_3, ..., x_{16}], x \in R^{16} \tag{2}$$

Each vector corresponds to a target value of the grasping force, $z \in R^{16}$. The goal of data processing is to establish the relationship between EMG signals and grasping force. Let $z = f(x)$.

4.2. Implementation of gene expression programming algorithms

Gene Expression Programming Algorithms (GEP) is a new adaptive evolutionary algorithm based on biological gene structure and expression process [53–55]. It is a robust variant of genetic algorithms (GA) and genetic programming (GP) [56,57]. GEP not only absorbs the advantages of GA and GP, but also overcomes their shortcomings. It has the characteristics of compact and stable coding structure, simple and effective genetic operation. The algorithm is faster and more accurate [58–60]. The biggest advantage is that it can solve complex problems by simple coding. The specific steps of GEP process are as follows:

(a) First, the population is initialized, and a certain number of individual sets are randomly generated as the initial population.
(b) Then we should calculate the fitness of each body in the population, and determine whether the fitness meets the calculation accuracy requirement or whether the number of iterations reaches the maximum evolution algebra. If one of them is satisfied, the evolution ends, and the output saves the optimal individual. Otherwise the next step is continued.
(c) Finally, according to the size of fitness value, the probability of being selected with large fitness is high, and the probability of being selected with small fitness value is low. A series of genetic operations, such as replication, mutation, insertion and recombination, are used to obtain the new population and recalculate its fitness. Loop in turn. The flow chart of the algorithm is shown in Fig. 7.

The grasping force prediction model based on GEP algorithm is constructed as follows:

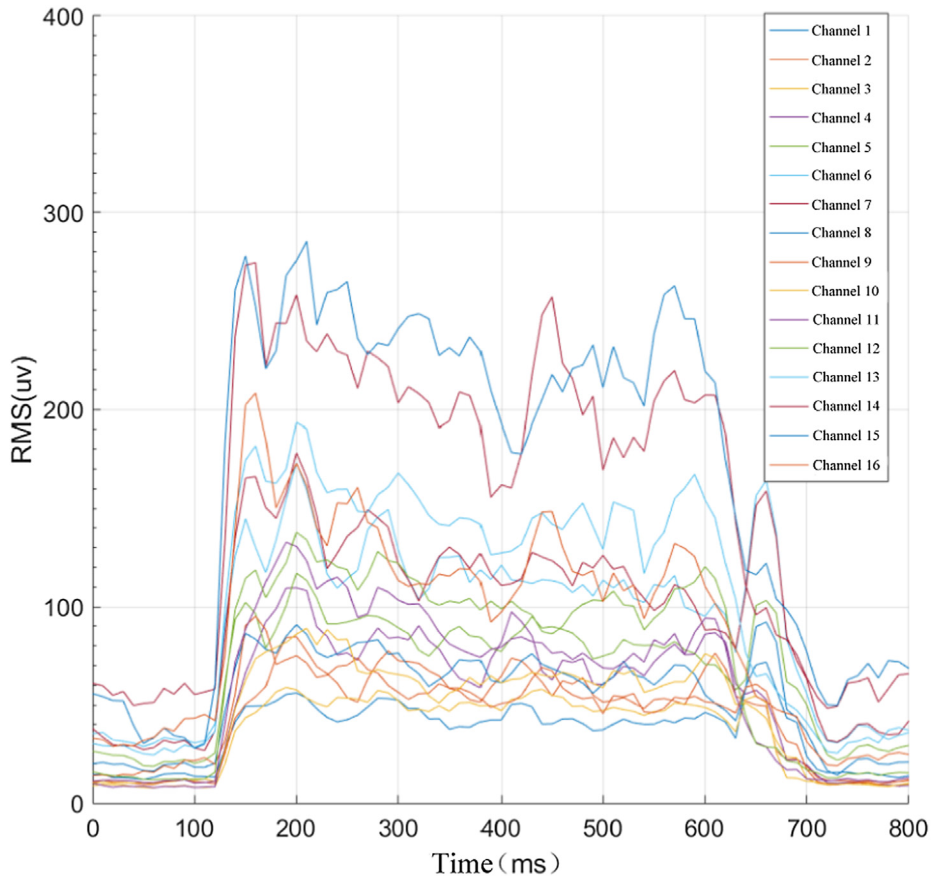

Fig. 4 40%MVC.

Input: RMS eigenvalue of sEMG signals [x_1-x_{16}], population number, gene length, gene number, mutation rate, insertion rate and recombination rate.

Output: optimal chromosome and corresponding predictive force function model.

Two termination criteria are defined: (i) the maximum number of iterations is 2000; (ii) Mean square error value (MSE) is less than 0.01. If any condition is met, the algorithm stops. The specific steps are as follows:

(a) The RMS eigenvalue sample set of sEMG signals is T. And the sliding window width is w which is included in T. The last $w-1$ data is added to the GEP parameter variable, and the remaining data is added to the predicted value list. The window slides in a unit width. A new $w$column data is formed.

(b) According to GEP algorithm, chromosomes are initialized, parameters are set, GEP-related coding is carried out, and population is formed.

(c) The fitness function should be calculated. Load the data set, and use the MSE of the training sample as the fitness value. The maximum fitness function is set to 1000. The fitness calculation is as shown in Eqs. (3) and (4).

$$f_{fitness} = 1000 \times \frac{1}{MSE_i + 1} \tag{3}$$

$$MSE_i = \frac{1}{m}\sum_{j-1}^{m}\left(F_{ij} - T_j\right) \tag{4}$$

where MSE_i represents the sum of mean square error, m is the total number of training samples, $F_{ij}$is the actual measured force in the equations, and T_j is the input of the sEMG signals. Predictive force is calculated by GEP Model. When $F_{ij} = T_j$, the fitness function is the largest and the prediction result is the most accurate.

Determine whether the optimal individual fitness value of the new generation population meets the requirements and preserve the optimal chromosome. If the condition is met, skip to (g). Otherwise, proceed to the next step.

(d) The genetic rules such as selection, replication, mutation, insertion and recombination are operated. The genetic rules are selected according to the standard roulette rules, and the best individuals are retained according to the elite retention strategy.

(e) Form the next generation of new individuals. First, the fitness values of new chromosomes that have been selected to undergo crossover and mutation operations are calculated. Then the chromosomes corresponding to these new parameter sets are combined with other chromosomes of the previous generation to form a new generation of chromosomes.

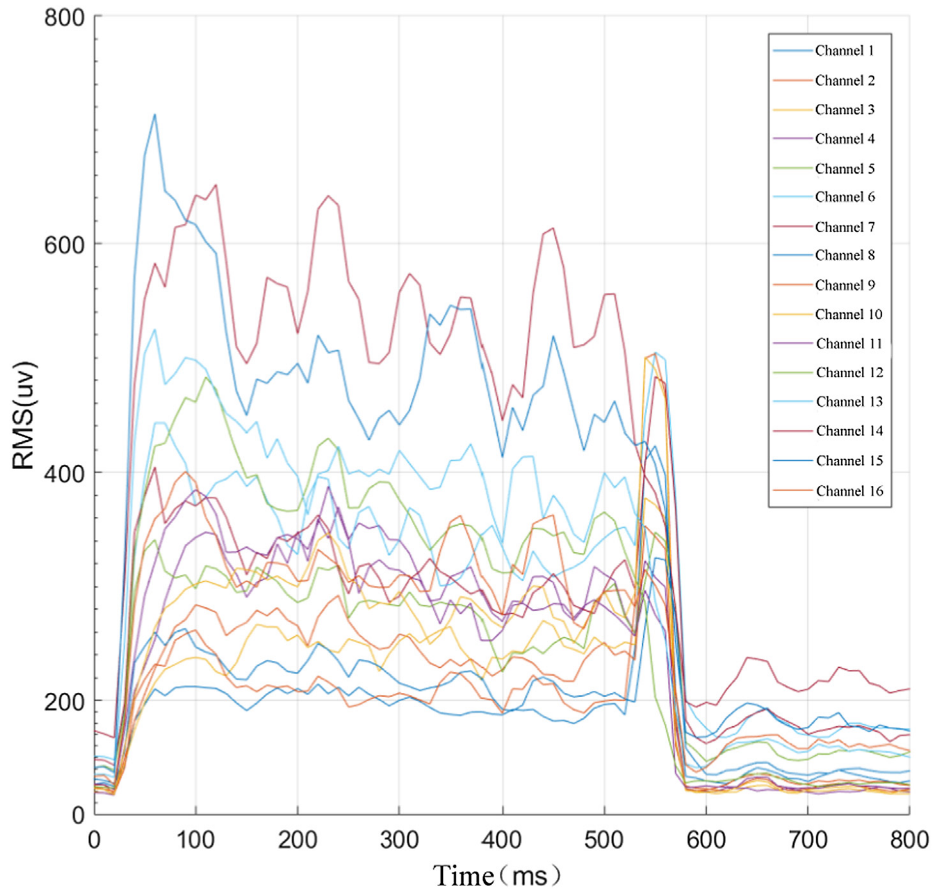

Fig. 5 60%MVC.

(f) The new individual is assessed for fitness by Eq. (2). Determine whether the optimal individual fitness value in the new generation population meets the expected requirements. If so, output the result and go to step (g). Otherwise, repeat the new population and return to step (d).
(g) When the optimal solution is found or the iteration step is reached, the operation terminates. Set two termination criteria: $f_{fitness} = f_{\max}$ and maximum algebra up to 2000. Determine whether the above criteria are met before each operation. If any criterion is met, the optimization process ends, the GEP operation is terminated, the grasping force prediction model function $F(x)$ is obtained, and the calculation result is output. Specific parameters are shown in Table 1.

Using the forecasting model constructed above, the fitness function $f_{fitness} = 997.627$ and $MSE = 0.0006$ can be obtained by running the program. According to the GEP algorithm decoding method, the input is the RMS eigenvalue of the sEMG signals of each channel, and the output is the corresponding grasping force prediction model function expression.

4.3. Realization of BP neural network algorithms

BP neural network is a kind of multi-layer neural network with three or more layers in structure. The most widely used is a three-layer neural network which is composed of input layer, hidden layer and output layer [54,55]. In this structure, the first and last layers are the input layer and the output layer respectively, and the middle layers are hidden layers. Each layer is composed of several neurons. The neurons in the left and right layers connect with each other, but there is no connection between the neurons in the upper and lower layers [61,62]. The network structure is shown in Fig. 8.

Where X_i is the input vector, i.e. the eigenvalue of the sEMG signals, R_j is the output vector of the hidden layer, Y_k is the actual output vector of the output layer, i.e. the predicted grasping force, W_{ij} is the connection weight of the input layer to the hidden layer, and W_{jk} is the connection weight of the hidden layer to the output layer [63,64].

According to the structure and basic theory of BP neural network, the algorithm steps and parameters of building BP neural network model for grasping force prediction are as follows.

(a) Weight initialization: randomly assign a small set of non-zero values to the weight.
(b) Determine the parameters of BP neural network and the definition of each variable: X_i is the input vector. Y_K is the actual output after the nth iteration of BP algorithm.
(c) The input S_j and output b_j of each neuron in the hidden layer are calculated. Enter S_j calculation formula as follows.

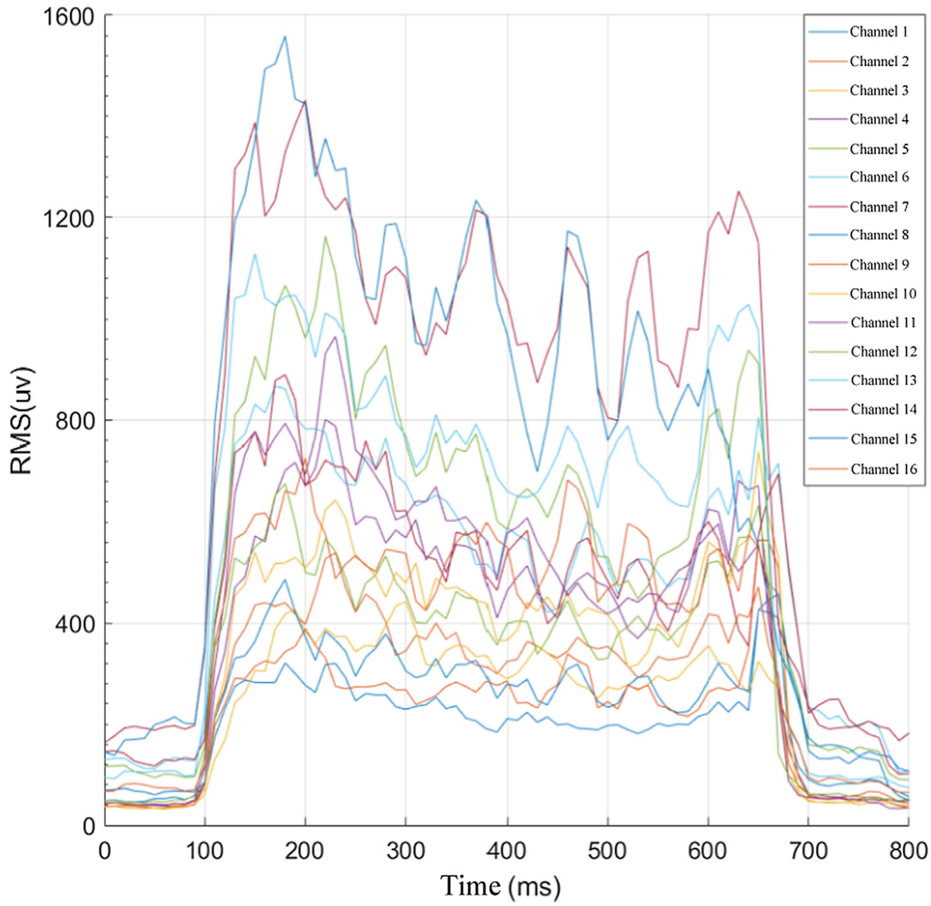

Fig. 6 80%MVC.

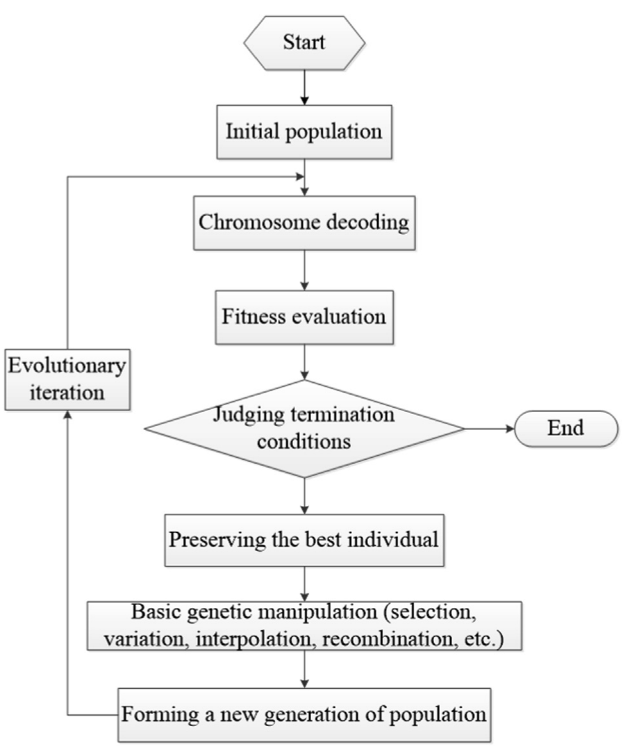

Fig. 7 Flow chart of GEP algorithm.

Table 1 GEP algorithm parameter settings.

Parameter	Value
Population size	200
Evolutionary algebra	2000
Number of genes	6
Mutation probability	0.045
Insertion /root insertion string transformation probability	0.1
Genetic transformation probability	0.1
Single point/Two point reorganization probability	0.2
Genetic recombination probability	0.1
Selection strategy	Roulette
Connection symbol	+
Fitness function	MSE

$$S_j = \sum_{i=1}^{n} w_{ij} \cdot X_i - \theta_j, (j = 1, 2, 3, ..., p) \quad (5)$$

$$f(x) = \frac{1}{1 + e^{-x}} \quad (6)$$

$$b_j = f(S_j) = \frac{1}{1 + \exp\left(-\sum_{i=1}^{n} w_{ij} \cdot X_i + \theta_j\right)} \quad (7)$$

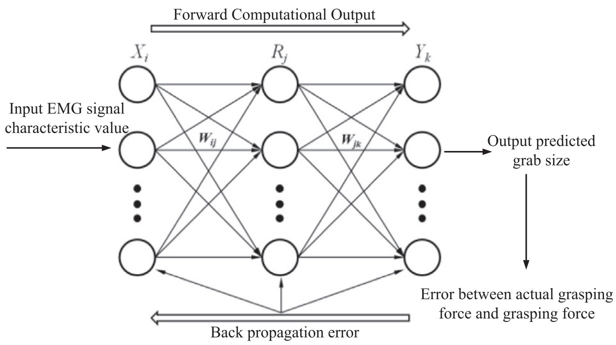

Fig. 8 Three-layer BP neural network structure model.

where w_{ij} represents the connection weight from the input layer to the hidden layer. X_i represents the characteristic value of the input EMG signal. θ_i represents the unit threshold of the hidden layer. n represents the number of neurons in the input layer. p represents the number of neurons in the hidden layer [65,66].

BP neural network prediction model is established based on the software of MATLAB R2013a to realize the prediction of sEMG signals grasping force. The number of hidden layer nodes is set to 21, the training function selects trainlm, the learning function selects leanngdm, the transfer function selects tansig, and the performance function selects MSE. After 30 iterations, $MSE = 0.0081$, less than 0.01, is obtained, and the training of prediction model is completed.

5. Experimental results and discussion

5.1. Evaluation index of force prediction effect

In order to measure the effect of force prediction, the root mean square error (RMSE) and cross-correlation (CC) criteria are used as indicators to evaluate the prediction results. The RMSE is a statistical measure of the performance of force prediction. It shows that the smaller the error between the predicted value and the actual value, the better. As shown in Eq. (8).

$$RMSE = \sqrt{\frac{1}{n}\sum_{1}^{n}(P_n - T_n)} \tag{8}$$

where P_n and T_n are the predicted value and the actual value of the grasping force respectively, and n is the number of samples. The CC is used to evaluate the similarity between the predicted value and the actual value. The closer the value is to 100, the higher the similarity. As shown in Eq. (9).

$$CC = \frac{cov(P,T)}{\sigma_p\sigma_t} \tag{9}$$

where $cov(P,T)$ is the covariance of the predicted value and the actual value, σ_p is the standard deviation of the predicted value and σ_t is the standard deviation of the actual value. In general, smaller RMSE value (close to 0) and a larger CC value (close to 1) indicate that the model has better generalization performance for force prediction.

5.2. Prediction and analysis of grasping force

Among the four hand grasping modes of G1–G4, five-fingered G4 has a wider application environment and demands in EMG prosthetic hand. So the hand grasping action is used to indicate the EMG signals and the grasping force under the G4 pinch. The data is experimental data used to compare the predictive force of different predictive models. By collecting multiple sets of 20% MVC, 40% MVC, 60% MVC and 80% MVC four levels of grasping force data, the mean and standard deviation are calculated and used as the target variables of the predictive model. The statistical results are shown in Table 2.

Under the five-finger pinch G4 grasping action, the RMSE and the CC obtained after the GEP algorithm prediction model and the BP neural network algorithm prediction model are used to train and predict the four different levels of grasping force. The statistical results are shown in Figs. 9 and 10.

For comparison, the data in the figure are expressed in the form of mean $\pm$ square difference.

It can be seen from Figs. 9 and 10 that the RMSE between the measured force and the predictive force obtained by the BP neural network algorithm and the GEP algorithm is less than 10%, and the CC is above 90%. However, from the overall data, the RMSE obtained by GEP algorithm is smaller and the CC is higher than that of BP neural network algorithm, which shows that GEP algorithm has higher CC. The prediction accuracy can better reflect the change of force. Four different levels of grasping force are predicted by GEP algorithm and BP neural network algorithm, and the predicted results are analyzed and compared, as shown in Figs. 11–14.

From Figs. 11–14, compared with BP neural network, the predicted result curve of GEP prediction model is closer to the target grasping force curve and has better fitting. In terms of the RMSE and the CC, the relative error and fluctuation of the GEP prediction model are smaller, which indicates that the prediction accuracy of the model is higher and the prediction results are more stable. The prediction results of individual locations are poor and the accuracy is not high, while the results of BP neural network prediction model are more accurate. GEP algorithm has the greatest prediction error and the

Table 2 Grasping force statistics under G4 grasping action of five fingers.

Grasping force grade	Min/N	Max/N	Mean/N	standard deviation /N
20%MVC	16	20	18	2.8
40%MVC	27	30	28.5	2
60%MVC	45	50	47.5	3.5
80%MVC	70	75	72.5	3.5
100%MVC	86	92	89	4

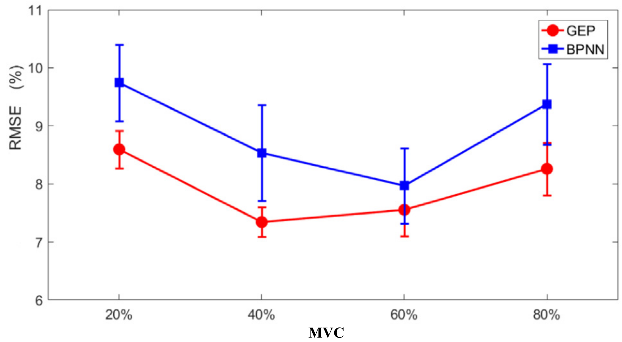

Fig. 9 Grasping Force Prediction RMSE Result Diagram.

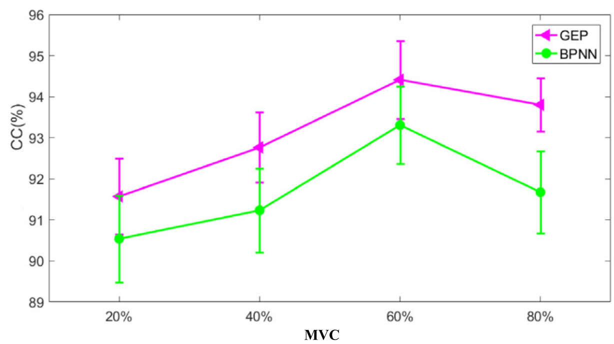

Fig. 10 Grasping Force Prediction CC Result Diagram.

lowest accuracy when the grasping force is 20% MVC. And the prediction accuracy is relatively high when the grasping force is 40% MVC, 60% MVC and 80% MVC. However, from the overall data point of view, the performance of GEP prediction model is better than that of BP neural network model. The reason is that GEP model has high mapping ability. Under the four grasping forces, GEP prediction model performs best, and with the improvement of grasping force, the prediction performance of GEP model tends to be good.

The above experimental results show that the RMSE value of the root mean square error of the grasping force predicted by GEP prediction model is the smallest 7.5%, the correlation coefficient CC is the largest 95%, the prediction accuracy is the highest and the result is the best when the grasping force level is 60% MVC. Further, in order to study the relationship between grasping mode and predicted grasping force, GEP prediction model is used to predict grasping force under four grasping action modes, and two evaluation indexes are obtained and compared. The results are shown in Figs. 15 and 16.

The experimental results show that the REMS of force prediction is the smallest and the CC is higher in the G1 grasping mode of thumb-index finger ($RMSE$ = 5.941 ± 0.188, CC = 95.562 ± 0.875). The force prediction result of the thumb-middle finger G2 grasping action is second ($RMSE$ = 6.585 ± 0.163, CC = 96.294 ± 0.934). Then the three-finger pinch grasping action G3 ($RMSE$ = 7.703 ± 0.178, CC = 94.741 ± 0.726). The force prediction result under the five-finger pinch grasping action G4 is relatively the worst ($RMSE$ = 8.588 ± 0.189, CC = 93.142 ± 1.125).

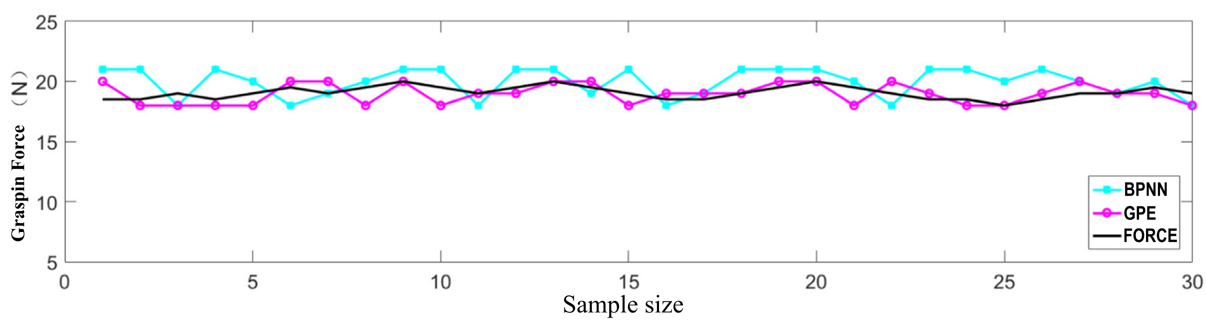

Fig. 11 Grasping force prediction result chart of 20% MVC.

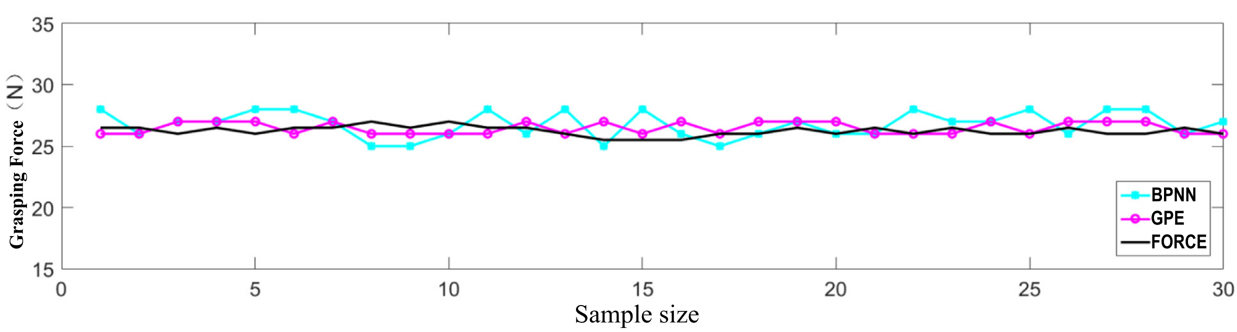

Fig. 12 Grasping force prediction result chart of 40% MVC.

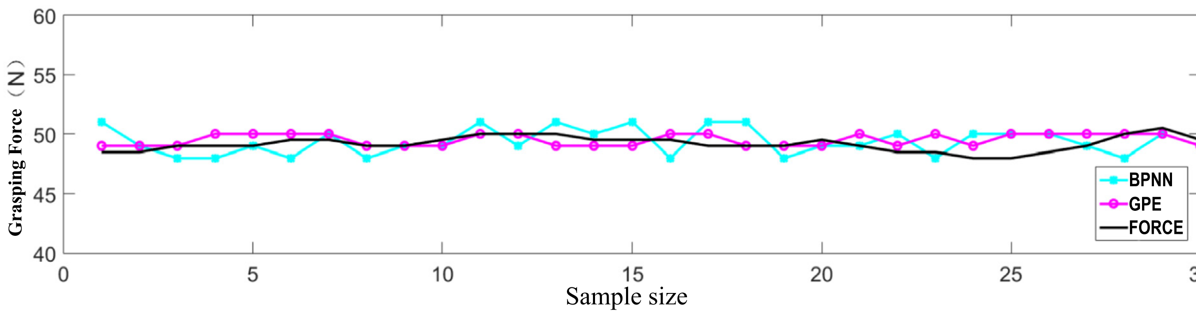

Fig. 13 Grasping force prediction result chart of 60% MVC.

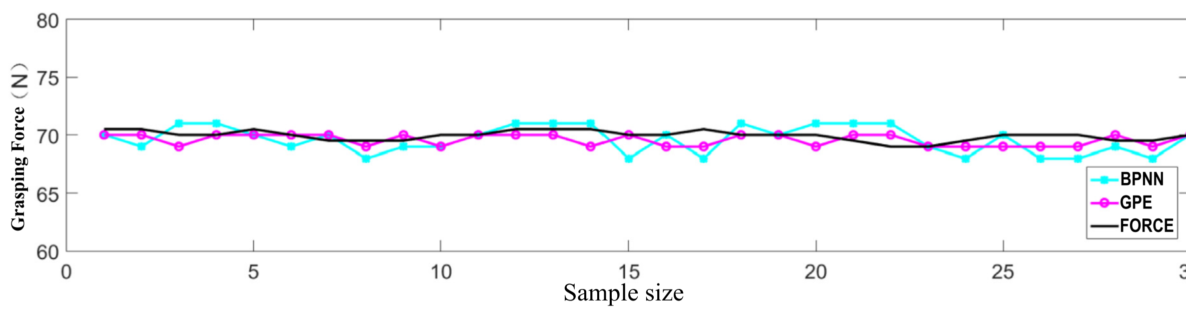

Fig. 14 Grasping force prediction result chart of 80% MVC.

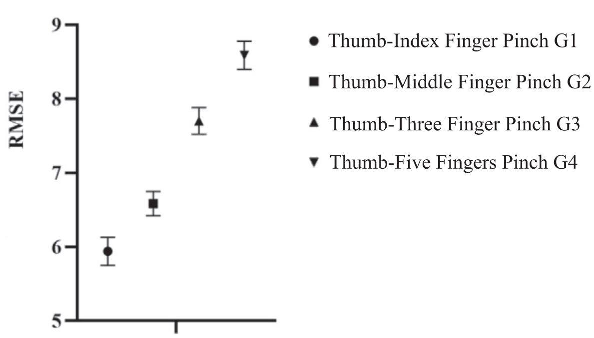

Fig. 15 The REMS of force prediction under four grasping modes.

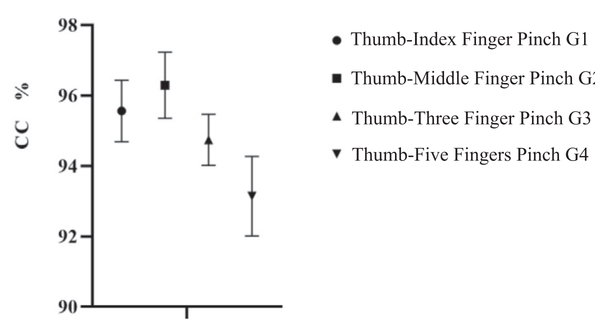

Fig. 16 Result of force prediction coefficient in four grasping modes.

The above experimental results show that the RMS of the time domain feature extracted from the sEMG signals can be used as a feature input sample to characterize the level of grasping force. The prediction model based on GEP algorithm can achieve the prediction of grasping force. Generally, the prediction accuracy is higher. However, as the grasping motion becomes more and more complex and the more fingers participate in the action, the force prediction error of the prediction model increases and the accuracy decreases.

6. Conclusion

The 16-channel electromyogram acquisition device is used to detect the EMG signals of hand grasping. Compared with the traditional electrodes, the prediction of grasping force can be achieved without precise positioning of EMG.

A grasping force prediction model based on GEP algorithm and BP neural network algorithm is constructed, and four different levels of grasping force are predicted. Through comparative analysis, it is found that the prediction error of grasping force based on GEP model is smaller than that based on BP neural network model, and the correlation coefficient value is higher, which shows that GEP algorithm has better prediction effect in grasping force prediction. GEP prediction model can be used to identify the grasping action and predict the grasping force, which can provide a solution to the problem of how to mine the force information in the muscle electrical signal to improve the flexible control of the prosthetic hand.

The RMS of time domain feature extracted from sEMG signals can be used as feature input samples to characterize the grasping force level. The prediction model based on GEP algorithm can realize the prediction of grasping force, and the prediction accuracy is high in general. However, as the grasping action becomes more and more complex and the more fingers participate in the action, the error of force prediction value of the prediction model is greater and the accuracy is reduced. It shows that the change of force has a certain impact on the stability of EMG prosthesis operation.

Acknowledgements

This research was supported by Hubei Provincial Department of Education (D20191105).

Declaration of Competing Interest

The authors declare that there is no conflict of interest regarding the publication of this article.

References

[1] M.A. Goodrich, A.C. Schultz, Human-robot interaction: a survey, Found. Trends Human-Comput. Interact. 1 (3) (2007) 203–275.
[2] Y. Nam, B. Koo, A. Cichocki, S. Choi, GOM-face: GKP, EOG, and EMG-based multimodal interface with application to humanoid robot control, IEEE Trans. Biomed. Eng. 61 (2) (2012) 453–462.
[3] F. Dario, H. Ales, Human-machine interfacing by decoding the surface electromyogram, IEEE Signal Process Mag. 32 (1) (2015) 115–120.
[4] J.X. Qi, G.Z. Jiang, G.F. Li, Y. Sun, T. Bo, Intelligent human-computer interaction based on surface EMG gesture recognition, IEEE Access 7 (2019) 61378–61387.
[5] N. Bandari, R. Ahmadi, A. Hooshiar, J. Dargahi, Hybrid piezoresistive-optical tactile sensor for simultaneous measurement of tissue stiffness and detection of tissue discontinuity in robot-assisted minimally invasive surgery, J. Biomed. Opt. 22 (7) (2017) 77002.
[6] C.C. Li, G.F. Li, G.Z. Jiang, D.S. Chen, H.H. Liu, Surface EMG data aggregation processing for intelligent prosthetic action recognition, Neural Comput. Appl. (2018), https://doi.org/10.1007/s00521-018-3909-z.
[7] Y.F. Fang, H.H. Liu, G.F. Li, X.Y. Zhu, A multichannel surface EMG system for hand motion recognition, Int. J. Humanoid Rob. 12 (2) (2015) 1550011.
[8] E.N. Kamavuako, D. Farina, W. Jensen, Estimation of grasping force from features of intramuscular EMG signals with mirrored bilateral training, Ann. Biomed. Eng. 40 (3) (2012) 648–656.
[9] G.F. Li, J.H. Li, Z.J. Ju, Y. Sun, J.Y. Kong, A novel feature extraction method for machine learning based on surface electromyography from healthy brain, Neural Comput. Appl. 31 (12) (2019) 9013–9022.
[10] T.S. Buchanan, D.G. Lloyd, K. Manal, T.F. Besier, Neuromusculoskeletal modeling: estimation of muscle forces and joint moments and movements from measurements of neural command, J. Appl. Biomech. 20 (4) (2004) 367–395.
[11] E.N. Kamavuako, D. Farina, K. Yoshida, W. Jensen, Estimation of grasping force from features of intramuscular EMG signals with mirrored bilateral training, Ann. Biomed. Eng. 40 (3) (2012) 648–656.
[12] Y. Sun, C.Q. Li, G.F. Li, G.Z. Jiang, D. Jiang, H.H. Liu, Z.G. Zheng, W.N. Shu, Gesture recognition based on kinect and sEMG signal fusion, Mobile Netw. Appl. 23 (4) (2018) 797–805.
[13] Z. Kappassov, J. Corrales, V. Perdereau, Tactile sensing in dexterous robot hands-review, Rob. Auton. Syst. 74 (2015) 195–220.
[14] K. Gui, H.H. Liu, D.G. Zhang, A Practical and adaptive method to achieve EMG-based torque estimation for a robotic exoskeleton, IEEE-ASME Trans. Mechatron. 24 (2) (2019) 483–494.
[15] J.S. Schofield, K.R. Evans, J.P. Carey, J.S. Hebert, Applications of sensory feedback in motorized upper extremity prosthesis: a review, Expert Rev. Med. Devices 11 (5) (2014) 499–511.
[16] G.F. Li, D. Jiang, Y.L. Zhou, G.Z. Jiang, J.Y. Kong, G. Manogaran, Human lesion detection method based on image information and brain signal, IEEE Access 7 (2019) 11533–11542.
[17] G.X. Ouyang, X.Y. Zhu, Z.J. Ju, H.H. Liu, Dynamical characteristics of surface EMG signals of hand grasps via recurrence plot, IEEE J. Biomed. Health. Inf. 18 (1) (2014) 257–365.
[18] C. Castellini, P.V.D. Smagt, Surface EMG in advanced hand prosthetics, Biol. Cybern. 100 (1) (2009) 35–47.
[19] D.G. Lloyd, T.F. Besier, An EMG-driven musculoskeletal model to estimate muscle forces and knee joint moments in VIVO, J. Biomech. 36 (6) (2003) 765–776.
[20] D. Gagnon, N. Arjmand, A. Plamondon, A. Shiraziadl, C. Lariviere, An improved multi-joint EMG-assisted optimization approach to estimate joint and muscle forces in a musculoskeletal model of the lumbar spine, J. Biomech. 44 (8) (2011) 1521–1529.
[21] G.F. Li, H. Wu, G.Z. Jiang, S. Xu, H.H. Liu, Dynamic gesture recognition in the internet of things, IEEE Access 7 (2019) 23713–23724.
[22] E. Scheme, K. Englehart, Electromyogram pattern recognition for control of powered upper-limb prostheses: state of the art and challenges for clinical use, J. Rehabil. Res. Dev. 48 (6) (2011) 643.
[23] A.H. Altimemy, R.N. Khushaba, G. Bugmann, Javier escudero, improving the performance against force variation of EMG controlled multifunctional upper-limb prostheses for transradial amputees, IEEE Trans. Neural Syst. Rehabil. Eng. 24 (6) (2015) 650–661.
[24] J.X. Qi, G.Z. Jiang, G.F. Li, Y. Sun, B. Tao, Surface EMG hand gesture recognition system based on PCA and GRNN, Neural Comput. Appl. (2019), https://doi.org/10.1007/s00521-019-04142-8.
[25] B.W. Luo, Y. Sun, G.F. Li, D.S. Chen, Z.J. Ju, Decomposition algorithm for depth image of human health posture based on brain health, Neural Comput. Appl. (2019), https://doi.org/10.1007/s00521-019-04141-9.
[26] X.C. Yang, X.L. Sun, D.L. Zhou, Y.F. Li, H.H. Liu, Towards wearable a-mode ultrasound sensing for real-time finger motion recognition, IEEE Trans. Neural Syst. Rehabil. Eng. 26 (6) (2018) 1199–1208.
[27] T.G. Chen, S.W. Wu, J.J. Yang, G.D. Cong, Risk propagation model and its simulation of emergency logistics network based on material reliability, Int. J. Environ. Res. Public Health 16 (23) (2019) 4677.
[28] J.B. Hu, Y. Sun, G.F. Li, G.Z. Jiang, B. Tao, Probability analysis for grasp planning facing the field of medical robotics, Measurement 141 (2019) 227–234.
[29] E.A. Clancy, N.E. Hogan, Probability density of the surface electromyogram and its relation to amplitude detectors, IEEE Trans. Biomed. Eng. 46 (6) (1999) 730–739.
[30] B.L. Liu, Z.J. Ju, H.H. Liu, A structured multi-feature representation for recognizing human action and interaction, Neurocomputing 318 (2018) 287–296.
[31] Y.F. Fang, D.L. Zhou, K.R. Li, H.H. Liu, Interface prostheses with classifier-feedback-based user training, IEEE Trans. Biomed. Eng. 64 (11) (2017) 2575–2583.
[32] C. Ferreira, Gene expression programming: a new adaptive algorithm for solving problems, Complex Syst. 13 (2) (2001) 87–129.

[33] W.T. Cheng, Y. Sun, G.F. Li, G.Z. Jiang, H.H. Liu, Jointly network: a network based on CNN and RBM for gesture recognition, Neural Comput. Appl. 31 (Supplement 1) (2019) 309–323.

[34] Y.J. Huang, X.C. Yang, Y.F. Li, D.L. Zhou, H.H. Liu, Ultrasound-based sensing models for finger motion classification, IEEE J. Biomed. Health. Inf. 22 (5) (2018) 1395–1405.

[35] J.P.M. Mogk, P.J. Keir, Crosstalk in surface electromyography of the proximal forearm during gripping tasks, J. Electromyogr. Kinesiol. 13 (1) (2003) 63–71.

[36] A. Erdemir, S.B. Mclean, W. Herzog, A.J. Van Den Bogert, Model-based estimation of muscle forces exerted during movements, Clin. Biomech. 22 (2) (2007) 131–154.

[37] D. Jiang, G.F. Li, Y. Sun, J.Y. Kong, B. Tao, Gesture recognition based on skeletonization algorithm and CNN with ASL database, Multimedia Tools Appl. 78 (21) (2019) 29953–29970.

[38] E. Scheme, K. Englehart, Electromyogram dynamical characteristics of surface EMG signals of hand grasps via recurrence plot pattern recognition for control of powered upper-limb prostheses: state of the art and challenges for clinical use, J. Rehabil. Res. Dev. 48 (6) (2011) 643–659.

[39] Y. Lu, Z.J. Ju, Y.R. Liu, Y.X. Shen, H.H. Liu, Time series modeling of surface EMG based hand manipulation identification via expectation maximization algorithm, Neurocomputing 168 (2015) 661–668.

[40] E.N. Kamavuako, D. Farina, K. Yoshida, W. Jensen, Relationship between grasping force and features of single-channel intramuscular EMG signals, J. Neurosci. Methods 185 (1) (2009) 143–150.

[41] K. Watanabe, M. Kouzaki, T. Moritani, Task-dependent spatial distribution of neural activation pattern in human rectus femoris muscle, J. Electromyogr. Kinesiol. 22 (2012) 251–258.

[42] C. Tan, Y. Sun, G.F. Li, G.Z. Jiang, D.S. Chen, H.H. Liu, Research on gesture recognition of smart data fusion features in the IoT, Neural Comput. Appl. (2019), https://doi.org/10.1007/s00521-019-04023-0.

[43] C.G. Taylor, R.J. Schwarz, The anatomy and mechanics of the human hand, Artificial Limbs 2 (2) (1955) 22–35.

[44] G.F. Li, L.L. Zhang, Y. Sun, J.Y. Kong, Towards the sEMG hand: internet of things sensors and haptic feedback application, Multimedia Tools Appl. (2018), https://doi.org/10.1007/s11042-018-6293-x.

[45] W.J. Chang, G.F. Li, J.Y. Kong, Y. Sun, G.Z. Jiang, H.H. Liu, Thermal mechanical stress analysis of ladle lining with integral brick joint, Arch. Metall. Mater. 63 (2) (2018) 659–666.

[46] M.C. Yu, G.F. Li, D. Jiang, G.Z. Jiang, B. Tao, D.S. Chen, Hand medical monitoring system based on machine learning and optimal EMG feature set, Pers. Ubiquit. Comput. (2019), https://doi.org/10.1007/s00779-019-01285-2.

[47] S.A. Nossier, M.R.M. Rizk, N.D. Moussa, S. Shehaby, Enhanced smart hearing aid using deep neural networks, Alexandria Eng. J. 58 (2019) 539–550.

[48] G.F. Li, H. Tang, Y. Sun, J.Y. Kong, G.Z. Jiang, D. Jiang, B. Tao, S. Xu, H.H. Liu, Hand gesture recognition based on convolution neural network, Cluster Comput. 22 (Supplement 2) (2019) 2719–2729.

[49] E. Yasser, Estimation and prediction of construction cost index using neural networks, time series, and regression, Alexandria Eng. J. 58 (2) (2019) 499–506.

[50] Y. Zhou, Y.F. Fang, K. Gui, K. Li, D.G. Zhang, H.H. Liu, Semg Bias-driven functional electrical stimulation system for upper-limb stroke rehabilitation, IEEE Sens. J. 18 (16) (2018) 6812–6821.

[51] M. Elkholy, M.M. Hosny, H.M.F. El-Habrouk, Studying the effect of lossy compression and image fusion on image classification, Alexandria Eng. J. 58 (1) (2019) 143–149.

[52] Y. He, G.F. Li, Y.Z. Zhao, Y. Sun, G.Z. Jiang, Numerical simulation-based optimization of contact stress distribution and lubrication conditions in the straight worm drive, Strength Mater. 50 (1) (2018) 157–165.

[53] M.C. Yu, G.F. Li, D. Jiang, G.Z. Jiang, F. Zeng, H.Y. Zhao, D. S. Chen, Application of Pso-Rbf neural network in gesture recognition of continuous surface EMG signals, J. Intelligent Fuzzy Syst. (2019), https://doi.org/10.3233/jifs-179535.

[54] D. Sedighizadeh, H. Mazaheripour, Optimization of multi objective vehicle routing problem using a new hybrid algorithm based on particle swarm optimization and artificial bee colony algorithm considering precedence constraints, Alexandria Eng. J. 57 (4) (2018) 2225–2239.

[55] W. Miao, G.F. Li, G.Z. Jiang, Y.F. Fang, Z.J. Ju, H.H. Liu, Optimal grasp planning of multi-fingered robotic hands: a review, Appl. Comput. Math. 14 (3) (2015) 238–247.

[56] Y. He, G.F. Li, Y.J. Liao, Y. Sun, J.Y. Kong, G.Z. Jiang, D. Jiang, H.H. Liu, Gesture recognition based on an improved local sparse representation classification algorithm, Cluster Comput. 22 (Supplement 5) (2019) 10935–10946.

[57] B. Li, Y. Sun, G.F. Li, J.Y. Kong, G.Z. Jiang, D. Jiang, B. Tao, S. Xu, H.H. Liu, Gesture recognition based on modified adaptive orthogonal matching pursuit algorithm, Cluster Comput. 22 (Supplement 1) (2019) 503–512.

[58] H.M. Shehata, Y.S. Mohamed, M. Abdellatif, T.H. Awad, Depth estimation of steel cracks using laser and image processing techniques, Alexandria Eng. J. 57 (4) (2018) 2713–2718.

[59] D. Jiang, G.F. Li, Y. Sun, J.Y. Kong, B. Tao, D. Chen, Grip strength forecast and rehabilitative guidance based on adaptive neural fuzzy inference system using sEMG, Pers. Ubiquit. Comput. (2019), https://doi.org/10.1007/s00779-019-01268-3.

[60] T.G. Chen, Q.Q. Li, J.J. Yang, G.D. Cong, G.F. Li, Modeling of the public opinion polarization process with the considerations of individual heterogeneity and dynamic conformity, Mathematics 7 (10) (2019) 917.

[61] L. Huang, Q.B. Fu, G.F. Li, B.W. Luo, D.S. Chen, H. Yu, Improvement of maximum variance weight partitioning particle filter in urban computing and intelligence, IEEE Access 7 (2019) 106527–106535.

[62] D. Jiang, Z.J. Zheng, G.F. Li, Y. Sun, J.Y. Kong, G.Z. Jiang, H. G. Xiong, B. Tao, S. Xu, H.H. Liu, Z.J. Ju, Gesture recognition based on binocular vision, Cluster Comput. 22 (Supplement 6) (2019) 13261–13271.

[63] Y.W. Cheng, G.F. Li, J.H. Li, Y. Sun, G.Z. Jiang, F. Zeng, H. Y. Zhao, D.S. Chen, Visualization of activated muscle area based on sEMG, J. Intell. Fuzzy Syst. (2019), https://doi.org/10.3233/jifs-179549.

[64] D.S. Chen, G.F. Li, Y. Sun, J.Y. Kong, G.Z. Jiang, H. Tang, Z. J. Ju, H. Yu, H.H. Liu, An interactive image segmentation method in hand gesture recognition, Sensors 17 (2) (2017) 253.

[65] Y.J. Liao, Y. Sun, G.F. Li, J.Y. Kong, G.Z. Jiang, D. Jiang, H. B. Cai, Z.J. Ju, H. Yu, H.H. Liu, Simultaneous calibration: a joint optimization approach for multiple kinect and external cameras, Sensors 17 (7) (2017) 1491.

[66] M.M. Alemi, J. Geissinger, A.A. Simon, S.E. Chang, A.T. Asbeck, A Passive exoskeleton reduces peak and mean EMG during symmetric and asymmetric lifting, J. Electromyogr. Kinesiol. 47 (2019) 25–34.